applied sciences

MDPI

Article

Predicting Swell in Clay-Sand Mixtures Used in Liners

Muawia Dafalla

Civil Engineering Department, King Saud University, Riyadh 11421, Saudi Arabia; mdafalla@ksu.edu.sa

Abstract: A method to predict the swellability of clay-sand mixtures is proposed. This model is a modified form of the Studds (1997) prediction model for clay-sand mixtures. The new proposed model uses the laboratory fall cone penetration technique to produce a characterization chart. This chart presents slope levels that can be used to obtain an equation for the final clay void ratio versus the vertical effective stress for clays. The porosity of the clay-sand mixtures was worked out based on a correction factor obtained from compression and porosity measurements in the laboratory. The porosity of the mixture was merged into the clay profile equation to compute the final clay void ratio at a specified stress level, which made it possible to predict the swelling behavior for different and variable stress levels. The swellability slope was obtained using fall cone tests conducted on the fine portion. Mixtures of kaolinite and bentonite were introduced to represent soils with different swell potentials. The fall cone measurements of a few points can be used to establish the swellability relationships for natural clay. Merging fall cone points with the swellability slope chart can define the profile of the vertical effective stress versus the clay void ratio.

Keywords: swelling; clay-sand mixtures; clay; effective stress; porosity

Citation: Dafalla, M. Predicting Swell in Clay-Sand Mixtures Used in Liners. *Appl. Sci.* **2023**, *13*, 11161. https://doi.org/10.3390/app132011161

Academic Editors: Xianwei Zhang, Xinyu Liu and Ran An

Received: 11 September 2023
Revised: 8 October 2023
Accepted: 9 October 2023
Published: 11 October 2023

1. Introduction

Studies on the identification and quantification of the swell in expansive clays, which have been carried out by many researchers, are either based on direct measurements of the swell potential and the swelling pressure or estimated from index properties. Most of the formulae established, if not all, are considered of local validity. These variations are mainly due to the different clay origins and mineralogical composition [1–3].

Field measurements and tests for such soils are very expensive and require long-term monitoring, which can extend to years. There is a lack of a simple field or laboratory test that can give reliable and informative results within a reasonably short period.

Geotechnical engineers are concerned about the increase and decrease in the volume of clays following wetting and drying. Bentonite is the name for commercial products that are rich in montmorillonite. Sodium Wyoming bentonite has received the greatest attention due to its ability to absorb large quantities of water and swell more than other types.

Modeling studies on the mechanical behavior of swelling clays and/or bentonite have been introduced by many researchers [4–10]. Understanding the mechanisms of volume changes helps to properly quantify and predict swelling behavior. It is quite common in the literature to come across terms of interlayer swelling, interparticle swelling, and interaggregate swelling. The first refers to the condition in which water is introduced between two layers of montmorillonite, causing the basal spacing to increase. This increase is variable and depends on the state of moisture. For dry commercial bentonite, the basal spacing increase is estimated to be in the order of 12.5 to 20 Å [9,11]. The interlayer swellings can double the volume of dry clay [12]. Interparticle swelling or osmosis is computed based on the double-layer theory, which uses the charge and spaces between particles. Interaggregate swelling occurs when aggregations and clusters are formed within the clay fabric.

The model proposed by Studds [11] for the prediction of the swelling behavior of bentonite–sand mixtures is an experimental approach suggesting the swell curve to be

presented in the form of the void ratio against the vertical effective stress. The model is generally based on three sets of data: the relationship between the clay void ratio (e_c) and the vertical effective stress (σ'_v) for bentonite with an appropriate permeant, the relationship between the sand porosity η_s and the vertical effective stress of the sand, and the sand porosity of the mixture in a dry state at an appropriate vertical effective stress. This approach is based on the concept of stress partitioning discussed by Mollins [9].

The clay void ratio concept used by Studds [11] and Mollins et al. [10] considers a two-phase sand–bentonite gel system (Figure 1). In this case, the clay is described in terms of the clay void ratio, defined as

$$e_c = \frac{Vw}{Vc} \tag{1}$$

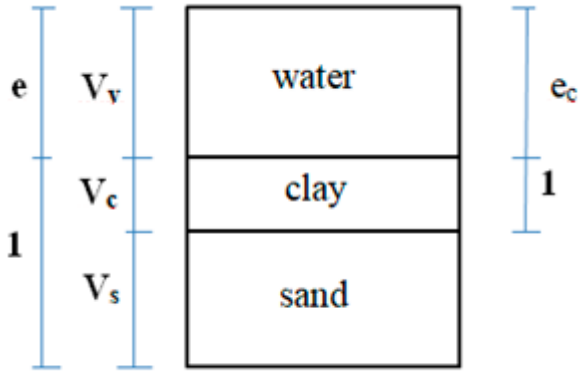

Figure 1. Phase diagram for saturated clay-sand mixture. *Vv* = volume of voids; *Vc* = volume of clay; *Vs* = volume of sand.

The conventional void ratio is shown on the left-hand side of the figure. The sand porosity is the total soil volume occupied by the paste and is given as

$$\eta s = \frac{(Vw + Vc)}{Vt} \tag{2}$$

where $Vt = Vw + Vc + Vs$.

Studds [11] assumed that the sand porosity of the dry mixture on a graph of η_s versus log σ'_v was parallel to the line of the pure sand but displaced from the compression line for the sand only. Studds proposed to obtain the sand porosity for a mixture at a given effective stress on the sand. This value was used to obtain the clay void ratio corresponding to the selected stress level via the following equation:

$$e_c = \frac{(\eta s(\text{mixture}) - x)}{x\,(1 - \eta s(\text{mixture})}} \tag{3}$$

where x is the volumetric fraction of clay in the mixture. This equation was derived by combining the following two equations:

$$e = e_c \cdot x \tag{4}$$

and

$$\eta s(\text{mixture}) = \frac{(e + x)}{(1 + e)} \tag{5}$$

The effective vertical stress applied to the clay can be found when the clay void ratio related to the selected stress level is obtained. By adding up the vertical effective stress on the sand and the vertical effective stress of clay, we can obtain the vertical effective stress of the mixture.

This method enables the clay void ratio of the mixture versus the vertical effective stress to be plotted. The final clay void ratio can be used to compute the material void ratio using the relationship given in Equation (4). The percentage volume change or swellability at a given effective stress can be predicted accordingly. This model is designed to obtain quick assessment based on simple fall cone tests.

2. Materials and Methods

2.1. Materials

2.1.1. Natural Clay

The natural clay material used in this study was obtained from the Tabuk region, towards the northwest of Saudi Arabia. These soils belong to a semiarid region and are subjected to cycles of repeated wetting and drying. The problems related to swelling in this region are of great concern to residents and local government authorities. Although the Tabuk clay is categorized as low-expansion clay, it has severely harmed a number of engineering projects. Table 1 displays the soil's geotechnical parameters that were measured.

Table 1. The main physical properties of Tabuk clay.

Property	Average
Dry unit weight (kN/m^3)	20.4
Moisture content (%)	13.1
Liquid limit (LL) (%)	37
Plastic limit (PL) (%)	24
Plasticity index (PI)	13
Shrinkage limit (%)	21
Percent sand (%)	6.0
Passing 63-micrometer sieve (%)	81
Specific gravity	2.79
Swelling pressure (kN/m^2)	49
Compression index (Cc)	0.12
Angle of shearing resistance (φ)	22

2.1.2. Bentonite Material

Volclay Ltd. (london, UK) supplied the bentonite clay that was utilized in this study. It had a specific gravity of 2.76, a liquid limit of 405%, and a plastic limit of 48%. The laboratory index property tests were performed in accordance with BS1377 Part 2, 1990 [13]. The findings of the chemical examination of the bentonite material are shown in Table 2.

Table 2. Volclay bentonite chemical analysis.

Chemical Analysis	Percentage by Weight
SiO_2	63.02
Al_2O_3	21.08
Fe_2O_3	3.25
Na_2O	2.57
MgO	2.67
CaO	0.65
FeO	0.35
Trace elements	0.72
Loss of ignition	5.64
Total	99.95

2.1.3. Kaolinite Material

Processed kaolinite can have slightly variable chemical and physical properties depending on the nature of the processing applied to natural clay. Table 3 presents a typical chemical composition for a kaolinite sample.

Table 3. Typical chemical composition of kaolinite.

Chemical Analysis	Percentage by Weight
SiO_2	48 +/− 0.1
Al_2O_3	36 +/− 0.1
Fe_2O_3	<0.75
MgO	<0.3
Na_2O	<1.0
K_2O	1.5 +/− 0.5
TiO_2	<0.5
L.O.I.	**12.5 +/− 0.5**

Kaolinite can have a viscosity of more than 30 kg/m.s and a thixotropy of less than 1.5 kg/m.s. The kaolinite generally used in this research was a product of the ECC International (Europe) Company. The product was Spess-White China Clay. The size distribution of the Spess-White China Clay kaolin, as tested by the manufacturer, indicated 78% clay and 22% silt. The following tests were performed for the China Clay in the laboratory, as per ASTM and/or British standards. The liquid limit was reported as 50% and the plastic limit was measured at 27%. The specific gravity of the Spess-White kaolinite was 2.50 and the computed activity was reported as 0.28.

Kaolinite is known as a material that has negligible swelling. The index properties measured indicate a classification of low to medium swelling. This classification is not valid. This supports the claim of Chen that all swelling clays have index properties as per the established classification and that a material does not need to have a high liquid limit or plasticity index to be a swelling material [2].

2.1.4. Sand Material

Natural wadi sand material obtained from a valley in Riyadh was used to produce the test soils. The properties of this type of sand are as follows:

Fines: Less than 2%.
Particle shape: Rounded to subangular.
Maximum grain size: 0.6 mm.
Uniformity: Poorly graded.
Specific gravity: 2.65.

The particle size distribution curve is shown in Figure 2.

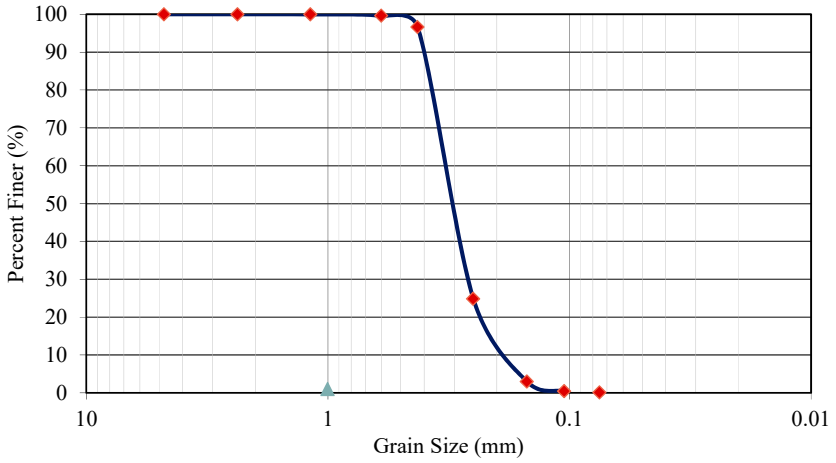

Figure 2. Grain size distribution for sand used in this study.

2.2. Testing Methods

2.2.1. The Fall Cone Test Method

This study's basic instrument was the penetrometer apparatus that is outlined in the British Standard (BS 1377: Part 2:1990:4.3) [13], which met the standards of BS 2000 Part 49.

The sample was cleansed of the particles that were retained on a 63 m test sieve. This was discovered to have an impact on the fall cone's penetration. For this test, the sample preparation technique was quite important. The fine-grained soil was vigorously combined using two palette knives for at least 10 min according to the British Standard to create a uniform paste. In order to avoid trapping air, a part of the mixed soil was forced into a normal cup or a ring with a 50 mm diameter and a 20 mm height. The cone was positioned such that its surface barely touched the sample, and it was then allowed to fall for five seconds. The original dial gauge readings before and after penetration were compared, and the difference was recorded to the nearest 0.1 mm.

The method used, as can be seen from the above description, is comparable to that for determining the liquid limit, with the exception of the preparation methods, which require that material with a particle size greater than 63 m be excluded. Additionally, when the penetration was less than 10 mm, the sample container was replaced with a 50 mm diameter by 20 mm high ring. Feng [14] discovered that a preparation method using specimen rings rather than cups was quicker and simpler. Additionally, he came to the conclusion that rings would lessen the possibility of the specimen accumulating air. The outcomes were found to be identical to those for the conventional cup.

For the fall cone method of determining the liquid limit, the test procedure was exactly as described above. A similar presentation of the data was used. A reduction in the impact of nonclay material on the penetration process can be achieved by rejecting material with a grain size greater than 63 m.

At various moisture contents, the test measured the penetration in mm. Semi-log charts can be used to display this relationship. Comparing the curve's trend with the curves of different materials is possible [15].

2.2.2. The Oedometer Testing Method

Using traditional oedometer techniques, tests for one-dimensional swelling were conducted. The sample was immersed in a container that enclosed a ring (the oedometer cell). Each sample had two porous disks at the bottom and top attached to Whatman filter sheets. This oedometer cell was housed inside a loading frame that transferred vertical loads via a uniquely crafted lever arm. Either a dial gauge with a precision of 0.01 mm or calibrated sensors that sense vertical movement were used to track changes in the sample height.

The utilized ring had a 50 mm diameter. A variable sample height was employed. The samples ranged in thickness from 3 to 8 mm. It was discovered that the initial swelling takes place more quickly in thin samples.

To estimate the swell parameters, one-dimensional swell testing was performed in accordance with ASTM D4546-96 method A [16]. The approach that deviates from this one uses a seating pressure of 7 kN/m^2. This technique involved submerging the sample and letting it swell vertically at the seating pressure for the duration of the principal swell. Similar procedures were used in the tests with various vertical effective stresses.

The ring's weight as well as the sample's weight were calculated. The sample's original height was noted. The initial moisture content and specific gravity were computed. These made it possible to calculate the height of the solids, Hs:

$$Hs = \frac{Ws}{A \cdot Gs \cdot \gamma_w} \quad (6)$$

The initial void ratio e_o was computed using the following formula:

$$e_o = \frac{\mathrm{H} - \mathrm{Hs}}{\mathrm{Hs}} \tag{7}$$

The change in the void ratio can be measured at any stage of the test in a similar fashion. Thus, the final void ratios at the end of the test are given as

$$e_f = \frac{\mathrm{H} - \mathrm{Hs}}{\mathrm{Hs}} \tag{8}$$

where Gs is the specific gravity, W_s is the dry weight of the sample, and γ_w is the density of water. The degree of saturation is given as

$$\mathrm{Sr} \cdot \ e \ = \mathrm{wGs} \tag{9}$$

where w is the moisture content.

Similar procedures were used for the oedometer tests conducted on remolded samples, bentonite powder, and mixes.

The samples were given time to air dry. In order to create a paste with a known moisture level, distilled water was added. If the dry density is known, the amount of soil required to fill the consolidation ring can be calculated. The calculated amount was tamped into the ring in two or three lifts.

The final clay void ratio was obtained from the pretest conditions as above, e_1, and the post-test parameters, e_2, using the following equation:

$$1 + e_2 \ = \frac{\mathrm{Gs}\gamma_w}{\gamma_d} \tag{10}$$

where γ_d is the dry unit weight.

This confirmed the accuracy of the data observed and recorded.

The final void ratio was taken as the average of e_1 and e_2. The surcharge or vertical effective stresses used varied from 1.96 to 400 kPa. This range covered the needs of geotechnical practice.

2.2.3. Samples Selected for Clay-Sand Mixture Prediction

The clay paste, which included only 40% bentonite by weight, was tested for penetration for the characterization of clay using the fall cone method. The corresponding clay void ratio versus the vertical effective stress was obtained based on the slope of the fall cone test chart.

Artificial clay consisting of 40% bentonite and 60% kaolinite was added to natural sand to form three different clay-sand mixtures. The clay was taken as 20%, 40%, or 80% according to the weight of the sand.

2.3. Modifications of the Studds Prediction Model

The use of the fall cone to characterize swelling clays enabled the construction of a chart that defines different swelling zones. This chart introduces lines of similar slopes to the vertical effective stress versus the final clay void ratio. The slope of the swellability line can be found when the slope of the moisture versus penetration in the chart is known. This can replace the testing required by Studds to obtain the final clay void ratio versus the effective stress. Using direct measurements to obtain the final clay void ratio normally takes several days. The set of equations for the vertical effective stress versus the clay void ratio is related to the specific fall cone profile. These can be used and the intermediate points can be worked out by interpolation.

The second modification was made to adjust the porosity factor of the clay-sand mixture adopted by Studds [11], which is valid only for bentonite and cannot be used

when kaolinite material is introduced. A new correction chart based on the inclusion of a non-swelling clay component was established. Figure 3 presents the new chart.

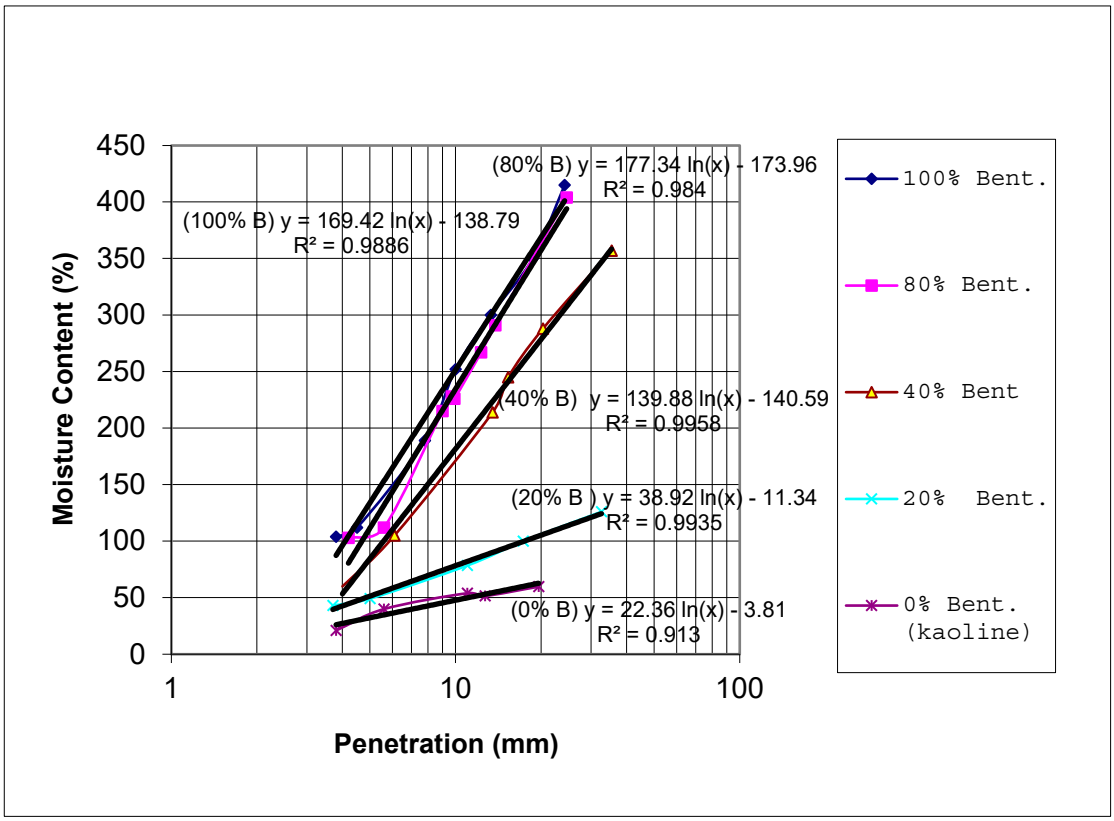

Figure 3. Idealized penetration chart for bentonite–kaolin mixtures.

The third modification of this system was to consider the silt material as part of the volumetric clay fraction (all material passing test sieve No. 200). This was implemented because, when measuring the shearing strength, the sample preparation technique for the fall cone includes this part. The attempt to include the silt within the clay for a specific purpose is not new. The authors of reference [17] considered all non-sand material as clay when investigating the liquid limit and the linear mixture law. The sand mixture porosity ($\eta_{s(mixture)}$) is given in Equation (5).

This value was calculated based on pretest dry conditions. When substituting for x, the silt material passing sieve No. 200 was included as a clay fraction.

Using the above modifications and assumptions, it was possible to predict the behavior of mixtures including sand, bentonite, and kaolin.

3. Results

Identification Tests

The test results obtained for the fall cone method were used to construct the chart presented in Figure 3. The clay void ratio versus the vertical effective stress for the selected bentonite–kaolin mixtures is presented in Figure 4. No prediction formula is given for the pure kaolinite in Figure 4. The laboratory porosity measurements carried out using the oedometer apparatus are presented in Figures 5 and 6. Trends in the artificial clay-sand mixtures are shown in Figure 7.

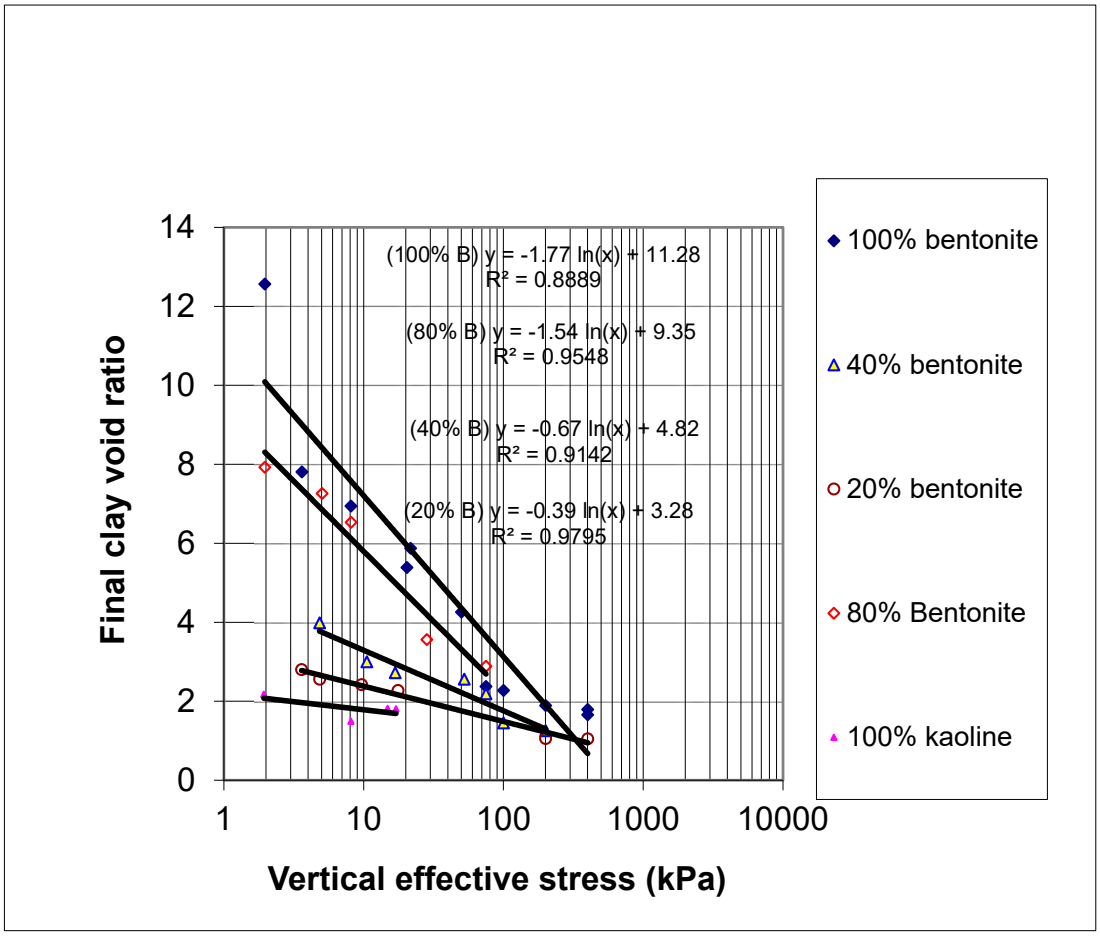

Figure 4. Final clay void ratio versus vertical effective stress for bentonite–kaolin mixtures.

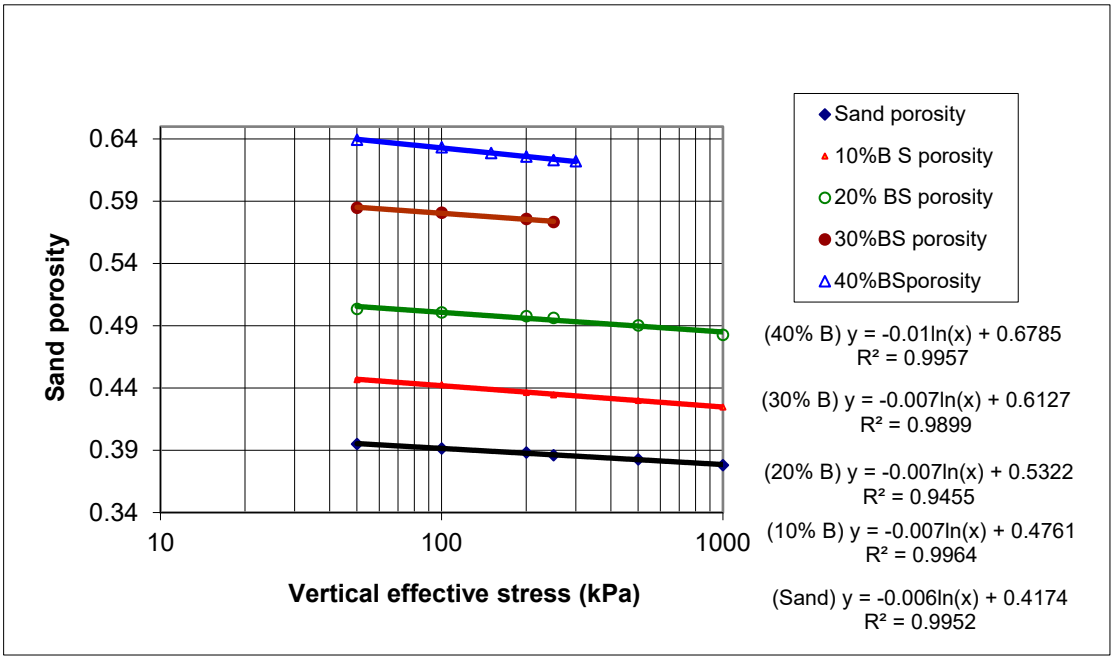

Figure 5. Compression and porosity of sand and sand with bentonite additives.

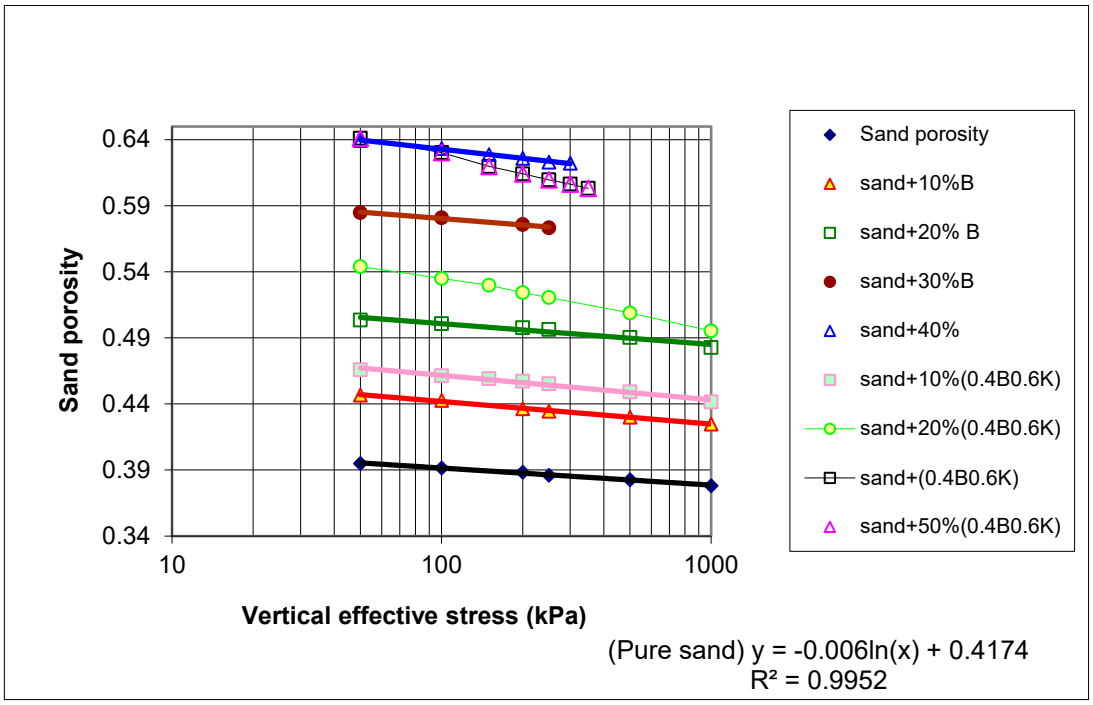

Figure 6. Compression and porosity of sand and sand with bentonite/kaolin additives.

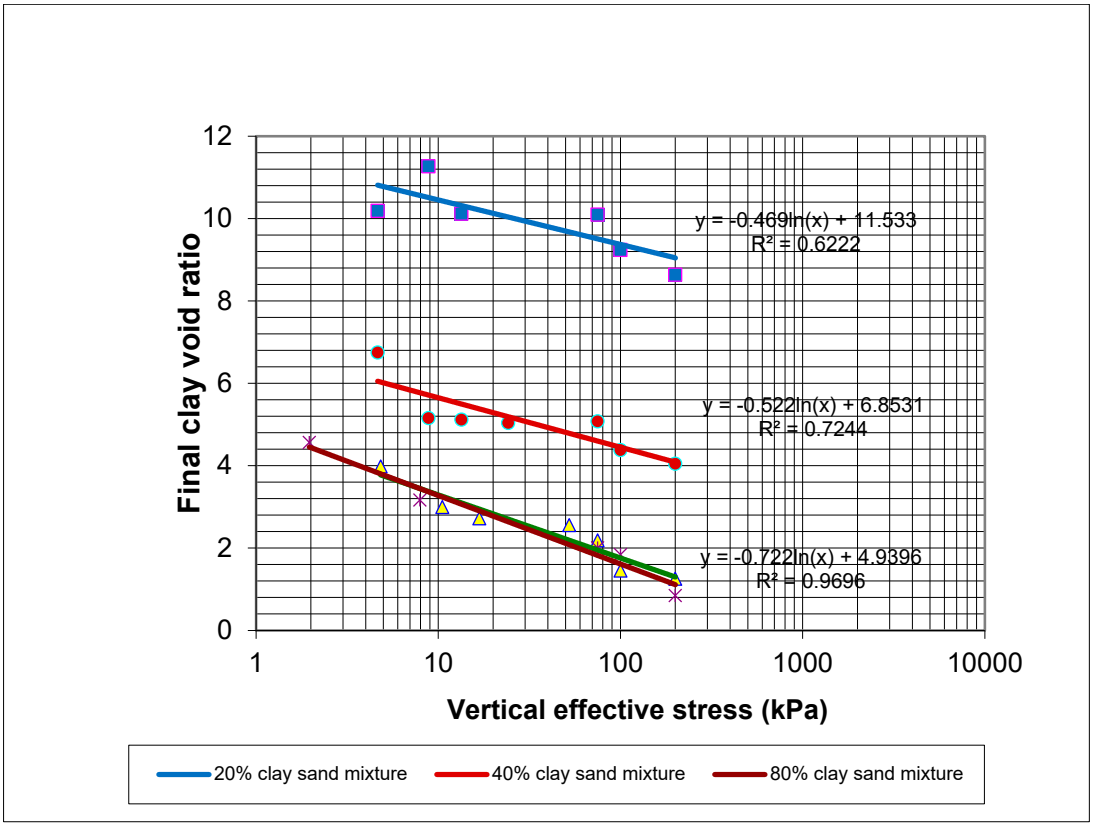

Figure 7. Vertical effective stress versus final clay void ratio for artificial clay-sand mixtures. (Green line is the reference bentonite material).

It is well known that index properties such as the liquid limit and plastic limit are used to roughly estimate the swelling of clay. These properties are strength-based parameters. The fall cone is a strength-measuring device ([18,19]). Therefore, it is expected to be very

useful in serving the goals of this research. The authors of reference [20] stated that the act of penetration by the fall cone provides a strength measurement that can indicate the compressibility of the soil.

4. Discussion

4.1. Final Clay Void Ratio and Equilibrium

Equilibrium is the state after which no change in the void ratio occurs when swelling clays are in saturated or near-saturated conditions. Expansion problems associated with saturated soils or originally wet soils are minimal. Initially, dry or partially saturated swelling clays are likely to cause structural problems following a moisture increase. The prediction of the compressibility and expansion of partially saturated soils is a cumbersome and difficult analysis that requires knowledge of several parameters. Mollins [8] found that the compaction method does not affect the final clay void ratio of samples. This study presents the clay void ratio versus the vertical effective stress for selected artificial soils using bentonite and kaolin mixtures.

Fine-grained soil water systems are commonly defined by the liquid and plastic limits. These are strength-based moisture contents. The free swell limit is defined as the maximum water-holding capacity of clayey soils and corresponds to a stress-free reference state. In this research, the term final clay void ratio is frequently quoted. This is the state at which the clay reaches equilibrium in a state similar to a stress-free reference state.

4.2. Prediction of the Swelling Behavior of Clay

Many factors, including the mineralogical composition, fabric, stress history, placement conditions, and geologic mode of the formation of the clay, influence the swelling behavior of naturally occurring clays. This prediction method assumes that the active constituents of natural clay give similar results as for remolded clays. Material with a similar amount of active clay compacted to variable densities will swell to a maximum level and maintain the same slope of swellability. The actual swell profile of natural clay may indicate a shift or slight displacement. The slope of the clay void ratio versus the vertical effective stress for the natural clay is obtained as a function of the slope predicted for the fine clay constituents using the fall cone method. However, the study of artificial and remolded clay is necessary to understand how these minerals behave when subjected to a moisture increase, which forms a useful guide for predicting the swell behavior of mixtures. Artificial mixtures are more common in the waste containment and liner industries.

The proposed prediction is based on obtaining the clay void ratio versus the vertical effective stress from the slope of relevant artificial clay. To achieve this, it is necessary to run a single or a few fall cone tests to establish the slope of swellability.

The clay paste, which included only 40% bentonite by weight, was tested for penetration for the characterization of clay using the fall cone method. The profile of the clay void ratio versus the vertical effective stress was obtained for the same material. The predicted equation for this type of clay (shown in Figure 4) is given by the following:

$$e_c = -0.6656\, ln\ \sigma c' + 4.824 \qquad R^2 = 0.9142 \tag{11}$$

4.3. Prediction of the Swelling Behavior of Clay-Sand Mixtures

Clay can be found in nature in the form of pure clay or clay intermixed with sand, silt, or other nonclay material (usually discrete inclusions). A clay paste is formed when water in the mixture combines with the clay. The "clay paste" can be either too little in volume and not sufficient to fill up the pores between the coarse component or available in large quantities to fill all the available voids. Most of the stresses are taken by the sand or coarse part in the first condition, and are not likely to be of major concern. For the second condition, the stress is shared and the response of the mixture depends on many factors, such as the stress–strain properties of the assemblage of coarse particles, voids within the system, and the type of clay. It is well understood that adding sand to clay improves the

shearing strength of the system. Additionally, it contributes indirectly by accelerating the consolidation of the slurry (Tan et al., 1994). It has also been found that the addition of sand to clay material affects the permeability of the mixture and helps with the quicker drainage of water.

Artificial clay consisting of 40% bentonite and 60% kaolinite was added to natural sand to form three different clay-sand mixtures. The clay was taken as 20%, 40%, or 80% according to the weight of sand.

The clay-sand mixture with 20% clay was tested for the effective stress and clay void ratio relations. The results measured in the laboratory are comparable to the data predicted by the Studds modified method. Table 4 presents how to calculate the final clay void ratio for different stress levels. The third column computes the porosity of the mixture at the given stress and as obtained from a direct test in the laboratory. The clay void ratio was computed and is presented in the fourth column. The stress of clay, which produces the same clay void ratio, is presented in a separate column. The stress exerted on the sand can be obtained by subtracting the stress on the clay from the total stress applied. The clay void ratio for the mixture was computed.

Table 4. Prediction table: clay-sand ratio of 0.2.

Stress Level (kPa)	Clay %	Porosity η	Void Ratio e_c	ln $\sigma'_{v\ clay}$	$\sigma'_{v\ clay}$ (kPa)	Stress on Sand $\sigma'_{v\ sand}$ (kPa)	e_c (mix)
2	0.2	0.597	4.931	−0.161186	0.851	1.1489	12.328
4	0.2	0.586	4.659	0.248376	1.281	2.7181	11.647
50	0.2	0.544	3.78	1.567824	4.796	45.204	9.451
100	0.2	0.533	3.567	1.888987	6.613	93.387	8.917
200	0.2	0.521	3.363	2.194884	8.979	191.021	8.408
300	0.2	0.515	3.248	2.367175	10.667	289.333	8.121
400	0.2	0.510	3.169	2.486579	12.020	387.980	7.922
500	0.2	0.507	3.108	2.577623	13.166	486.834	7.771
600	0.2	0.504	3.059	2.651015	14.168	585.832	7.649
700	0.2	0.501	3.019	2.71238	15.065	684.935	7.547
1000	0.2	0.495	2.926	2.852011	17.323	982.677	7.314

Table 4 indicates that sands contribute to taking some of the load from very low stresses. The portion taken by clay reduces upon increasing the applied load. This becomes insignificant for extremely high loads. The clay can fill up the voids of the sand and push the sand grains apart. This action causes the sand porosity to increase. When pressure is exerted on clay, it compresses to a smaller volume, making the sand less porous.

The clay-sand mixture with 40% clay by weight tested similarly, and yielded the results presented in Table 5.

Table 5. Prediction table: clay-sand ratio of 0.4.

Stress Level (kPa)	Clay %	Porosity η	Void Ratio e_c	ln $\sigma'_{v\ clay}$	$\sigma'_{v\ clay}$ (kPa)	Stress on Sand $\sigma'_{v\ sand}$ (kPa)	e_c (mix)
2	0.4	0.7062	2.606	3.332896	28.019	−26	6.514
4	0.4	0.6924	2.377	3.676886	39.523	−35.5	5.942
50	0.4	0.6422	1.692	4.705966	110.610	−60.6	4.229
100	0.4	0.6284	1.536	4.939705	139.730	−39.7	3.840
200	0.4	0.6146	1.392	5.156714	173.590	26.4	3.479
400	0.4	0.6008	1.257	5.358727	212.450	188	3.1430
500	0.4	0.5963	1.216	5.420823	226.070	274	3.040
600	0.4	0.5927	1.183	5.470554	237.59	362	2.957
800	0.4	0.587	1.132	5.547247	256.53	543	2.829
1000	0.4	0.5825	1.093	5.605286	271.86	728	2.733

It can be noted from Table 5 that the clay carried all the low stresses. The model shows that the stresses acting on the sand were negative. This results from the use of the clay profile equation over the full range. The points showing negative values reflect the theoretical figures so that all assumptions hold. This method can show when the sand starts to contribute to taking up stresses. This point is defined by Mollins as the threshold point. It can be graphically determined if the void ratio versus the effective stress profile of the clay-sand mixture intersects the profile of clay.

The clay-sand mixture with 80% clay was entirely governed by the behavior of the clay. The results of the measured clay void ratio were found to coincide with those of the clay alone (40% bentonite). For this case, the prediction model used the equation for the clay. This finding has been reported by many authors, including Mollins [8] and Studds [11].

Kumar and Wood [20] found that, for a clay content above 35%, the clay matrix alone controlled the mechanical behavior of the mixture. This value is for a clay–gravel mixture and for a particular clay material, which is kaolinite. However, when investigating the dry powder effect on the porosity of the coarse material, it can be observed that the shift in the porosity line is large compared with that in the original line of the coarse material only. Pure bentonite clay tested by Mollins [8] showed that a clay content as small as 10% could control the behavior of a mixture until a certain point of stress. This is the threshold point mentioned above. The clay content at which the entire mechanical behavior is controlled by the fine part depends on the type of clay, the porosity of the coarse material, and the stress level.

The authors of reference [21] regarded the sand as an inert filler and the clay phase as determining the swelling of clay-sand mixes. This is not necessarily true; the coarse material also has a role in the way clay can expand. The porosity and geometry of sand grains can influence the quantitative behavior of the clay paste.

Studies conducted to investigate the characteristics and shear strength behavior of clay-sand mixtures, in general, include the works in references [22–24]. In reference [25], it is stated that the clay content in clayey sand has a significant influence on the stress–strain profile of the soil mass. As the fine content increased, the dilatant behavior of the clayey sand decreased and the response gradually became similar to that of clay-like material at about 40% fine content. The authors of reference [26] experimentally studied the behavior of clay-sand mixtures under compression and extension triaxial loading paths. Reference [23] reports that the shear strength properties and the stress–strain characteristics of mixtures of sand–kaolin showed a significant change at a kaolin content of 20%. In a study in reference [27], the authors performed a series of unconsolidated, undrained triaxial tests to evaluate the effects of some factors on the compacted bentonite–sand mixtures. These included the moisture, the energy of compaction, and the confining pressure in addition to the clay content. Sridharan and Prakash [28] claim that the liquid limit and the plastic limits cannot represent the plasticity limits and they do not correspond to stress-free reference states. They suggested three characteristic water contents, namely the free swell limit, the settling limit, and the shrinkage limit.

5. Conclusions

The clay void ratio versus the vertical effective stress for a clay material can be obtained by comparing the fall cone penetration data of the clay with the slope obtained for artificial clay. The chart constructed for artificial clay using the fall cone can be used to characterize the swell potential of any given plastic to highly plastic clay.

The stress–strain behavior of the clay-sand mixture system is influenced by the behavior of each component. The independent responses of fine- and coarse-grained components can be useful for estimating stress portioning and predicting the overall behavior of the soil mass. The porosity compression relationship of the coarse part can be studied when the voids are partially filled up with fine material in a dry state. This was found to be comparable to the overall mixture behavior when wetted. The modified Studds model was suitable for predicting the clay void ratio versus the effective stress for 40% clay or less.

The clay-sand mixture with 80% clay was entirely governed by the behavior of the clay. The results of the measured clay void ratio were found to coincide with those of the clay alone.

Funding: This research was funded by the Deanship of Scientific Research of King Saud University. Researchers Supporting Project, number RSPD2023R1059.

Data Availability Statement: All data related to this manuscript are available upon request.

Acknowledgments: The author gratefully acknowledges the Researchers Supporting Project, number RSPD2023R1059, King Saud University, Riyadh, Saudi Arabia, for their financial support for the research work reported in this article.

Conflicts of Interest: The author declares no conflict of interest.

List of Symbols

Symbol	Description
e	Void ratio
e_c	Clay void ratio
e_f	Final void ratio
e_1	Pretest void ratio
e_2	Post-test void ratio
γ_d	Dry unit weight
σ'_v	Vertical effective stress
ηs	Sand porosity
$\eta s_{(mixture)}$	Sand porosity of mixture
x	Volumetric fraction of clay
Vw	Volume of water
Vc	Volume of clay
Vt	Total volume
H	Height of sample
Hs	Height of solids
Ws	Weight of solids
A	Area
Gs	Specific gravity
γ_w	Unit weight of water
Sr	Degree of saturation
w	Water content
LL	Liquid limit
PL	Plastic limit
PI	Plasticity index
Cc	Compression index
φ	Angle of shearing resistance
L.O.I.	Loss of ignition

References

1. Zein, A.K.M. Comparison of Measured and Predicted Swelling Behavior of a Compacted Black Cotton Soil. In Proceedings of the Sixth International Conference on Expansive Soils, New Delhi, India, 1–4 December 1987; pp. 121–126.
2. Chen, F.H. *Foundations on Expansive Soils*; Elsevier Scientific Publishing Company: Amsterdam, The Netherlands, 1988.
3. Dafalla, M.A.; Al-Sharmrani, M.A. Performance-Based Solutions For Foundations on Expansive Soils—Al Ghatt Region, Saudi Arabia. In Proceedings of the International Conference on Geotechnical Engineering, Chiangmai, Thailand, 10–12 December 2008.
4. Alonso, E.E.; Gens, A.; Josa, A. A constitutive model for partially saturated soils. *Géotechnique* **1990**, *40*, 405–430. [CrossRef]
5. Alonso, E.E.; Vaunat, J.; Gens, A. Modelling the mechanical behaviour of expansive clays. *Eng. Geol.* **1999**, *54*, 173–183. [CrossRef]
6. Gens, A.; Alonso, E.E. A framework for the behaviour of unsaturated expansive clays. *Can. Geotech. J.* **1992**, *29*, 1013–1032. [CrossRef]
7. Pusch, R.; Schomburg, J. Impact of microstructure on the hydraulic conductivity of undisturbed and artificially prepared smectitic clay. *Eng. Geol.* **1999**, *54*, 167–172. [CrossRef]

8. Mollins, L.H. The Design of Bentonite-Sand Mixtures. Ph.D. Thesis, University of Leeds, Leeds, UK, 1996.
9. Mollins, L.H.; Stewart, D.I.; Cousens, T.W. Predicting the properties of bentonite-sand mixtures. *Clay Miner.* **1996**, *31*, 243–252. [CrossRef]
10. Stewart, D.I.; Studds, P.G.; Cousens, T.W. The factors controlling the engineering properties of bentonite-enhanced sand. *Appl. Clay Sci.* **2003**, *23*, 97–110. [CrossRef]
11. Studds, P.G. The Effect of Ionic Solutions on the Properties of Soil. Ph.D. Thesis, University of Leeds, Leeds, UK, 1997.
12. Olphen, H.V. *An Introduction to Clay Colloid Chemistry, for Clay Technologists, Geologists, and Soil Scientists*; Interscience Publishers: Hoboken, NJ, USA, 1977.
13. *BS 1377-2:1990*; Methods of Test for Soils for Civil Engineering Purposes. Classification tests. British Standards Institution: London, UK.
14. Feng, T.W. Fall-cone penetration and water content relationship of clays. *Géotechnique* **2000**, *50*, 181–187. [CrossRef]
15. Dafalla, M.A. The Use of the Fall Cone Penetrometer in the Characterization and Assessment of Swelling Clays. Ph.D. Thesis, University of Leeds, Leeds, UK, 2004.
16. *ASTM D4546-96*; Standard Test Methods for One-Dimensional Swell or Settlement Potential of Cohesive Soils. ASTM International: West Conshohocken, PA, USA, 1996.
17. Tan, T.S.; Goh, T.-C.; Kuranaratne, G.P.; Lee, S.L. Shear strength of very soft clay-sand mixtures. *Geotech. Test. J.* **1994**, *17*, 27–34.
18. Wood, D.M. Some Fall Cone Tests. *Geotechnique* **1985**, *3*, 64–68. [CrossRef]
19. Wood, D.M.; Worth, C.P. The use of Cone Penetrometer to Determine the Plastic Limit of Soils. *J. Ground Eng.* **1978**, *11*, 37.
20. Kumar, G.V.; Muir Wood, D. Fall cone and compression tests on clay-gravel mixtures. *Geotechnique* **1999**, *49*, 727–739. [CrossRef]
21. Dixon, D.A.; Gray, M.N.; Thomas, A.W. A study of the compaction properties of potential clay-sand buffer mixtures for use in nuclear fuel waste disposal. *Eng. Geol.* **1985**, *21*, 247–255. [CrossRef]
22. Chalermyanont, T.; Arrykul, S. Compacted sand-bentonite mixtures for hydraulic containment liners. *Songklanakarin J. Sci. Technol.* **2005**, *27*, 313–323.
23. Olmez, M.S. Shear Strength Behavior of Sand-Clay Mixtures. Master's Thesis, Middle East Technical University, Ankara, Turkey, 2008.
24. Gueddouda, M.K.; Goual, I.; Lamara, M.; Aboubaker, N. Hydraulic Conductivity and Shear Strength of Compacted Dune Sand-Bentonite Mixtures. In Proceedings of the International Conference on Construction and Building Technology (ICCBT 2008), Kuala Lumpur, Malaysia, 16–20 June 2008; pp. 139–150.
25. Georgianou, V.; Burland, J.; Hight, D. The undrained behavior of clayed sands in triaxial compression and extension. *Geotechnique* **1990**, *41*, 383–393. [CrossRef]
26. Shafiee, A.; Tavakoli, H.R.; Jafari, M.K. Undrained behavior of compacted sand-clay mixtures under monotonic loading paths. *J. Appl. Sci.* **2008**, *8*, 3108–3118. [CrossRef]
27. Chen, Y.; Meehan, C.L. Undrained strength characteristics of compacted bentonite-sand mixtures. In *Geo-Frontiers 2011-ASCE, Geotechnical Special Publications (GSP) 211*; Han, A., Ed.; ASCE Library: Reston, VA, USA, 2011; pp. 2699–2708.
28. Sridharan, A.; Prakash, K. The characteristic water content of fine grained soil-water system. *Geotechnique* **1998**, *48*, 337–346. [CrossRef]